

Pamukkale Üniversitesi Mühendislik Bilimleri Dergisi

Pamukkale University Journal of Engineering Sciences



Evaluation of Sliding mode control algorithms for load frequency control of a single area power system

Tek bölgeli bir güç sisteminin yük frekans kontrolü için kayan kipli kontrol algoritmalarının değerlendirilmesi

Ali Efe Olcay1*, Murat Furat1

¹Iskenderun Technical University, Iskenderun, Hatay, Türkiye. ali.olcay.lee22@iste.edu.tr, murat.furat@iste.edu.tr

Received/Geliş Tarihi: 18.03.2025 Accepted/Kabul Tarihi: 30.08.2025 Revision/Düzeltme Tarihi: 18.07.2025 doi: 10.5505/pajes.2025.26109 Research Article/Araştırma Makalesi

Abstract

This study deals with the evaluation of load frequency control (LFC) by sliding mode controllers (SMC), which have two different structures. As the LFC is one of the significant problems of power systems, there have been many solutions proposed for this problem, especially based on the well-known PID controller. The SMC is an effective alternative that has been focused on for power systems. Therefore, two recently popular SMC algorithms are evaluated for the LFC of a single-area power system. One algorithm is model-based, first-order SMC, and the other one is a modelfree, second-order super-twisting SMC algorithm smoothed with a hyperbolic tangent function. Optimization of the controllers is performed with two metaheuristic algorithms, the Sine Cosine Optimization Algorithm (SCA), and the Grey Wolf Optimizer (GWO). The controllers' performance is evaluated for an applied 0.1pu load. Detailed results are given in tabulated form and graphically.

Keywords: Load Frequency Control, Sliding Mode Control, Sine Cosine Optimization, Grey Wolf Optimizer

Ör

Bu çalışma, yük frekans kontrolünün (YFK) iki farklı yapıya sahip Kayan Kipli Kontrol (KKK) ile değerlendirilmesini ele almaktadır. YFK güç sistemlerinin önemli problemlerinden biri olduğundan, bu problem için özellikle iyi bilinen PID kontrolörüne dayalı birçok çözüm önerilmiştir. KKK, güç sistemleri için üzerinde durulan etkili bir alternatiftir. Bu nedenle, son zamanlarda popüler olan iki KKK algoritması tek alanlı bir güç sisteminin YFK için değerlendirilmiştir. Algoritmalardan biri model tabanlı, birinci dereceden KKK, diğeri ise hiperbolik tanjant fonksiyonu ile yumuşatılmış, modelsiz, ikinci dereceden süper bükümlü SMC algoritmasıdır. Kontrolörlerin optimizasyonu iki meta sezgisel algoritma olan Sinüs Kosinüs Optimizasyon Algoritması ve Gri Kurt Optimize Edici ile gerçekleştirilmiştir. Kontrolörlerin performansı uygulanan 0.1pu yük için değerlendirilmiştir. Detaylı sonuçlar tablo halinde ve grafiksel olarak verilmiştir.

Anahtar kelimeler: Yük Frekans Kontrolü, Kayan Kipli Kontrol, Sinüs Kosinüs Optimizasyonu, Gri Kurt Optimize Edici.

1 Introduction

In electric power systems, maintaining a stable and reliable frequency is a critical factor for ensuring continuous and balanced operation. Load variations in the grid can disrupt the balance between generation and consumption, leading to frequency fluctuations. To prevent these fluctuations and keep the system at its nominal frequency, Load Frequency Control (LFC) plays a crucial role. LFC's primary objective is to keep power exchange and frequency within the desired limits across various regions [1]. Load frequency control is based on continuously monitoring the system frequency and detecting deviations. When there is a deviation in the frequency, it generates an error signal. An appropriate control input is produced since the error signal is fed into the control system to recover the disturbed frequency. Consequently, LFC represents one of the key challenges for power systems.

Türkiye operates in synchronization with the European Union (EU) as part of the European Network of Transmission System Operators for Electricity (ENTSO-E). The nominal frequency in both Türkiye and the EU is 50 Hz. However, generation modules must continue to operate even when deviations from the nominal frequency occur. For example, in the European continent, they are expected to remain in the system within the 49.0 Hz to 51.0 Hz range without any time limitation. For other frequency ranges, specific operational duration requirements

have been established. For instance, generation modules must be capable of operating for at least 30 minutes within the 47.5 Hz to 48.5 Hz frequency range [2]. In Türkiye, the nominal system frequency is regulated by the Turkish Electricity Transmission Corporation (TEIAS) within the range of 49.8-50.2 Hz. TEIAS and user equipment must be designed to operate continuously within the 49.0-51.0 Hz range and for at least 30 minutes within the 47.5-48.5 Hz range or 51.0-51.5 Hz range [3].

The controller design is of great importance for load frequency control applications. Optimized PID controllers remain widely used in industry due to their simplicity and efficiency [4]. Nevertheless, numerous scholars have noted in the literature that PID adjustments made with traditional methods lack robustness, prompting investigations into new controller designs. [5]. Therefore, there are a lot of proposed methods for load frequency control systems in literature such as sliding mode control (SMC) [6], [7], [8], [9], [10], [11], [12], [13], fractional-order PID [14], [15], fractional-order fuzzy PID [16], and internal model control (IMC) [5], [17]. Various studies in the literature demonstrate that the SMC method provides an effective solution for load frequency control. This method has been successfully applied to single-area (SAPS), two-area (TAPS), and multi-area power systems (MAPS) by incorporating different optimization algorithms. For instance, in a MAPS, a Particle Swarm Optimization (PSO)-based Sliding

1

^{*}Corresponding author/Yazışılan Yazar

Mode Control (PSOSMC) method has been proposed [9]. Another study demonstrated that SMC, when tuned with the Bees Algorithm (BA), exhibits superior performance compared to other controllers [10]. Similarly, for a SAPS, LFC has been implemented using the Sine Cosine Optimization Algorithm (SCA) [15]. Further literature analysis, the readers can refer these studies [18], [19], [20].

Although the conventional SMC provides robust control against parameter variations and disturbances in the controlled system, its main drawback is the chattering, which excites undesirable high-frequency dynamics [18]. The drawback is caused by the signum function in the control input and is overcome by replacing the smooth functions instead of the signum function [18], [19]. To alleviate chattering, Second-Order Sliding Mode Control (SOSMC) methods have been proposed as an alternative solution. For example, it has been stated that SOSMC reduces the chattering effect compared to classical SMC and the conventional PI controllers [7]. In another study, it was demonstrated that the Super-Twisting SMC (ST-SMC) outperforms the integral controller for the LFC in a TAPS [8].

In the present study, two recently proposed types of sliding mode control algorithms are evaluated for load frequency control of a SAPS. One is the conventional type of SMC based on a PID+D2 sliding surface [10], [13], [23], and the other is supertwisting SMC smoothed with a hyperbolic tangent function [24], [25]. According to the relative degree, the first one is a first-order SMC, in which system model parameters are used to construct the control input, and the other is a second-order SMC algorithm. To the best of our knowledge, the selected SMC algorithms are first evaluated for the LFC of SAPS. The parameters of both controllers are optimized with well-known metaheuristic algorithms.

The remainder of the paper is organized as follows. In section 2, the principle of load frequency control is explained. Then, the design principles of the selected SMC algorithms are given in detail in Section 3. The optimization algorithms are introduced in Section 4. Section 5 contains the results of the optimization and a related discussion. Section 6 includes the conclusion of the paper.

1.1 Load Frequency Control

LFC is crucial for the sustainable operation of power systems. LFC aims to ensure that the power generated matches the power demanded in the system, thus maintaining the frequency at its nominal level. A SAPS' LFC comprises a governor, a turbine, a generator, and a load.

As the real power systems consist of many complex parameters, linearized models have been frequently preferred in scientific studies. For example, IEEE recommended a linear excitation system model for power system stability studies [21]. Therefore, a linear model-based SAPS was selected from the previous studies to evaluate the performance of the SMC algorithms. Fig. 1 depicts the block diagram of a SAPS featuring linearized transfer functions.

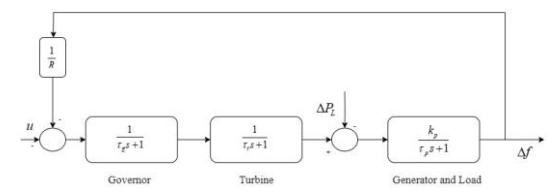


Figure 1. Single area power system block diagram

The whole transfer function between the control input and the frequency deviation at the output of the generator can be written as follows:

$$G(s) = \frac{k_p}{(\tau_p s + 1)(\tau_t s + 1)(\tau_g s + 1) + k_p/R}$$
 (1)

The parameters of the SAPS are shown in Table 1 [13].

Table 1. Parameters of the SAPS in Fig. 1

Description	Parameter	Value
Gain Constant of Power	k_{p}	120
System	P	
Time Constant of Power	$ au_p$	20
System	· p	
Time Constant of Turbine	$ au_t$	0.3
Time Constant of Governor	$ au_g$	0.08
Constant of Speed Regulation	$\overset{\circ}{R}$	2.4

When the parameters given in Table 1 are substituted into the transfer function given in Eq. (1), one has:

$$G(s) = \frac{120}{0.48s^3 + 7.62s^2 + 20.38s + 51}$$
 (2)

Eq. (2) can be simplified as:

$$G(s) = \frac{250}{s^3 + 15.88s^2 + 42.45s + 106.25}$$
 (3)

In the next section, the third-order transfer function, Eq. (3), is used in the sliding mode controller design as:

$$G(s) = \frac{A}{s^3 + Bs^2 + Cs + D} \tag{4}$$

2 Sliding Mode Controllers' Design

SMC was introduced to the international literature by Utkin in 1977 [23]. Since then, sliding mode controllers have been commonly employed in industries because of their durability and reliable performance. This method, preferred for the control of nonlinear systems, is resistant to parameter uncertainties and external disturbances. However, one disadvantage of SMC is the occurrence of unwanted vibrations in the control input, known as "chattering," caused by high-frequency switching signals [18], [20], [24]. The control input generated by SMC consists of an equivalent control law, $u_{eq}(t)$, and a switching control law, $u_{sw}(t)$. While the equivalent control signal is sought in sliding surface function derivatives, the switching control signal is selected, taking into account the stability of the system. The control signal is then found as:

$$u(t) = u_{eq}(t) + u_{sw}(t) \tag{5}$$

2.1 PID+D² sliding surface-based controller

The control signal of the model-based SMC algorithms can be obtained with a few steps, as follows:

- Decide on a sliding surface function
- Obtain the equivalent control law using the system model
- Find ideal sliding mode
- Decide the switching control law that provides stability.

2.1.1 PID+D² sliding surface

In recent studies on power systems, PID+D 2 sliding surface-based controllers were proposed [10], [13], [20]. Therefore, in this study, this type of controller is selected for the evaluation, given in Eq. (6):

$$\sigma(t) = k_1 e(t) + k_2 \int e(t)dt + k_3 \frac{d}{dt} e(t) + k_4 \frac{d^2}{dt^2} e(t)$$
 (6)

where e(t) is the error in frequency, e(t) = r(t) - y(t), r(t) denotes reference and y(t) denotes output frequency deviation, Δf . Since $\Delta f = 0$ is desired, the error is $e(t) = 0 - \Delta f = -\Delta f$. The constants $k_1, k_2, k_3, k_4 \in \mathbb{R}^+$.

2.1.2 Equivalent Control Law

The control input based on the sliding surface in Eq. (6) is obtained by a number of derivation steps. The first step is to obtain inverse Laplace transform of the system model in Eq. (4):

$$\ddot{y}(t) = Cu(t) - A\ddot{y}(t) - B\dot{y}(t) - Dy(t) \tag{7}$$

Substituting Eq. (7) into $\ddot{e}(t) = \ddot{r}(t) - \ddot{y}(t)$ results in:

$$\ddot{e}(t) = \ddot{r}(t) + A\ddot{v}(t) + B\dot{v}(t) + Dv(t) - Cu(t) \tag{8}$$

As described in the previous section, the control input is sum of equivalent and switching control laws. The $u_{eq}(t)$, is sought in the derivatives of the sliding surface. For the selected sliding surface, in Eq. (6), its first-order derivative contains the control input. The first-order derivative of Eq. (6) is as follows:

$$\dot{\sigma}(t) = k_1 \dot{e}(t) + k_2 e(t) + k_3 \ddot{e}(t) + k_4 \ddot{e}(t) \tag{9}$$

The control input was found in the first-order derivative of the selected function for the system in Eq. (1), which is why it is referred to as first-order SMC or conventional SMC.

Substituting Eq. (8) into Eq. (9) gives:

$$\begin{split} \dot{\sigma}(t) &= k_1 \dot{e}(t) + k_2 e(t) + k_3 \ddot{e}(t) \\ &\quad + k_4 [\ddot{r}(t) + A \ddot{y}(t) + B \dot{y}(t) + D y(t) \ (10) \\ &\quad - C u(t)] \end{split}$$

The $u_{eq}(t)$ is obtained by equating Eq. (10) to zero:

$$u_{eq}(t) = \frac{1}{k_4 C} \left[k_1 \dot{e}(t) + k_2 e(t) + k_3 \ddot{e}(t) + k_4 [\ddot{r}(t) + A \ddot{y}(t) + B \dot{y}(t) + D y(t)] \right]$$
(11)

2.1.3 Ideal Sliding Mode

At this step of the derivation, $u(t) = u_{eq}(t) + u_{sw}(t)$

and $u_{eq}(t)$ is substituted into Eq. (10). Then, one can have the ideal sliding mode as follows:

$$\dot{\sigma}(t) = -k_4 C u_{sw}(t) \tag{12}$$

2.1.4 Switching Control Law

The last step involves selecting a switching control law that ensures stability. To achieve this, a positive definite Lyapunov function is chosen as follows:

$$V(t) = 0.5\sigma^2(t) \tag{13}$$

According to the theorem, derivative of Eq. (13) must be negative definite, as follows:

$$\dot{V}(t) = \sigma(t)\dot{\sigma}(t) < 0 \tag{14}$$

Since $\dot{\sigma}(t)$ is known, Eq. (12), one can find that:

$$\dot{V}(t) = -k_4 C \sigma(t) u_{sw}(t) \tag{15}$$

In the literature, switching control law is generally decided as a signum function with a constant, such as $u_{sw}(t) = k_{sw}(\sigma(t))$. Since $sgn(\sigma(t)) = |\sigma(t)|/\sigma(t)$, Eq. (14) becomes $\dot{V}(t) = -k_4C|\sigma(t)| < 0$. This results in a selected switching control law that makes the system stable.

Summing out both equivalent and switching control laws constitute the control input as:

$$\begin{split} u(t) = & \frac{1}{k_4 C} \left[k_1 \dot{e}(t) + k_2 e(t) + k_3 \ddot{e}(t) \right. \\ & \left. + k_4 (\ddot{r}(t) + A \ddot{y}(t) + B \dot{y}(t) + D y(t)) \right]^{\left(16\right)} \\ & \left. + k_{sw} sgn(\sigma(t)) \right. \end{split}$$

The sign function in Eq. (16) generates a highly oscillating control signal, namely, chattering. Therefore, it is smoothed by replacing it with the hyperbolic tangent function as [18]:

$$\begin{split} u(t) &= \frac{1}{k_4 C} \left[k_1 \dot{e}(t) + k_2 e(t) + k_3 \ddot{e}(t) \right. \\ &+ k_4 (\ddot{r}(t) + A \ddot{y}(t) + B \dot{y}(t) + D y(t)) \right]^{\left(17\right)} \\ &+ k_{sw} tanh(\sigma(t)) \end{split}$$

The block diagram of the PID+D² sliding surface-based controller is illustrated in Fig. 2.

2.2 Hyperbolic Tangent-based ST-SMC

where

The ST-SMC is a second-order sliding mode control method that provides continuous control signals. On the other hand, the algorithm needs knowledge of the sign of the sliding variable. In this study, the sliding variable is defined as the tracking error of the frequency deviation, $s(t) = r(t) - y(t) = -\Delta f$. Basically, the control input of the super-twisting algorithm is as follows [25]:

$$u_{st} = k_1 |s(t)|^{0.5} sgn(s(t)) + u_1(t)$$

$$u_1 = k_2 sgn(s(t))$$
(18)

In Eq. (18), k_1 and k_2 are gains of the controller, $k_1, k_2 \in \mathbb{R}^+$.

As stated in [25], the controller does not generate a smooth control input. Therefore, the following hyperbolic tangent-based ST-SMC algorithm [21], [22] is preferred in this study:

$$u_{st}=k_1|s(t)|^{0.5}tanh(s(t))+u_1(t) \label{eq:ust}$$
 where
$$u_1=k_2tanh(s(t)) \label{eq:ust}$$
 (19)

The block diagram of the hyperbolic tangent-based ST-SMC algorithm is illustrated in Fig. 3.

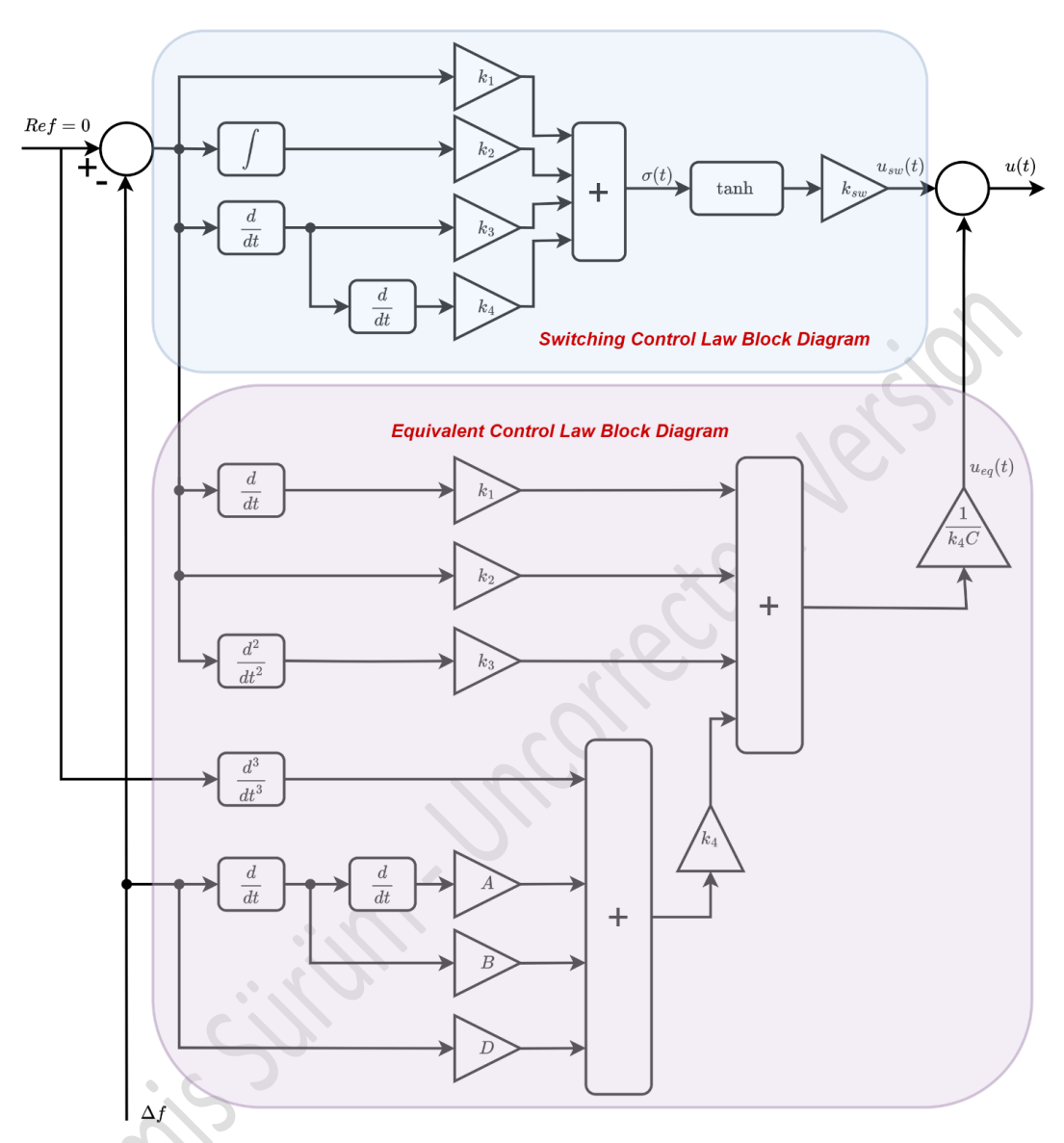


Figure 2. The PID+D² sliding surface-based SMC block diagram.

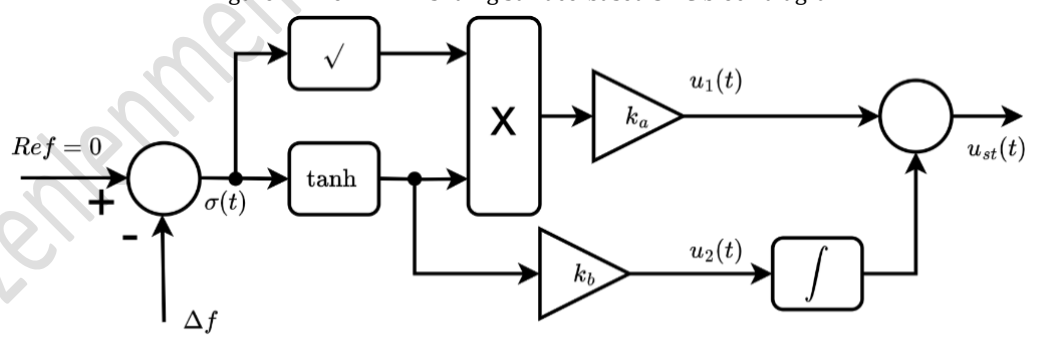


Figure 3. The hyperbolic tangent-based ST-SMC block diagram

3 Optimization Algorithms

The current study employs two metaheuristic optimization algorithms to investigate the optimal controller parameters described in the preceding section. Two of the optimization algorithms are SCA and GWO. Both algorithms are based on

population principles and investigate optimal values from predefined search spaces for each control parameter.

3.1 Sine Cosine Optimization Algorithm

The Sine Cosine Optimization Algorithm (SCA) was proposed by Seyedali Mirjalili. The algorithm attempts to find the optimal value using sine and cosine functions. It starts optimization

with an initial set of random candidates selected in the predefined search spaces. Then, it saves the best obtained data and updates other solutions accordingly [26]. The algorithm is based on the oscillation of sine and cosine functions including random variables, as follows:

$$X_i^{t+1} = \begin{cases} X_i^t + r_1 \times \sin(r_2) \times |r_3 P_i^t - X_i^t|, r_4 < 0.5 \\ X_i^t + r_1 \times \cos(r_2) \times |r_3 P_i^t - X_i^t|, r_4 \ge 0.5 \end{cases}$$
(20)

where X_i^t stands for the position of the current solution in i^{th} dimension at the t^{th} iteration, r_1, r_2, r_3 are random variables, P_i denotes the position of the destination point in the i^{th} dimension and r_4 is a random number in [0,1] [26].

The effects of Sine and Cosine in Eq. (20) are demonstrated in Fig. 4, and the flowchart of the SCA is illustrated in Fig. 5.

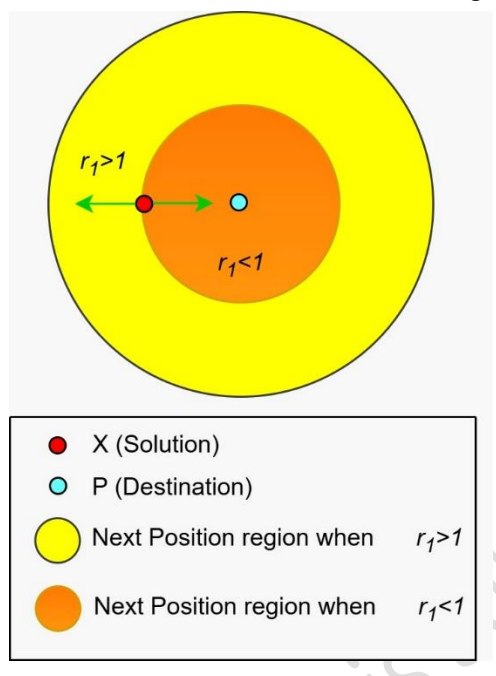


Figure 4. Effect of Sine Cosine in Eq. 20.

3.2 Grey Wolf Optimizer

The Grey Wolf Optimizer (GWO) is an optimization algorithm inspired by nature, designed to mimic the hunting strategies and social hierarchy of wolves. It was developed by Seyedali Mirjalili and his team in 2014 [27]. Grey wolves, which are thought to be at the top of the food chain and live in packs, are the model for the GWO, a swarm-based algorithm. The GWO algorithm's initial optimization step involves generating a random population of grey wolves, named as alpha, beta, and delta wolves, or potential solutions. The wolves make iterations to determine the prey's likely location. The distance between each possible solution and the prey is updated. When an end criterion is satisfied, the GWO algorithm is finally ended.

In the present study, the PID+D² sliding surface-based SMC and hyperbolic tangent-based ST-SMC are evaluated for the LFC of a SAPS. The optimization process is aimed at minimizing the integral of squared error (ISE), which is commonly preferred as a performance indicator in optimization problems. ISE is defined as:

$$ISE = \int e^2(t)dt \tag{21}$$

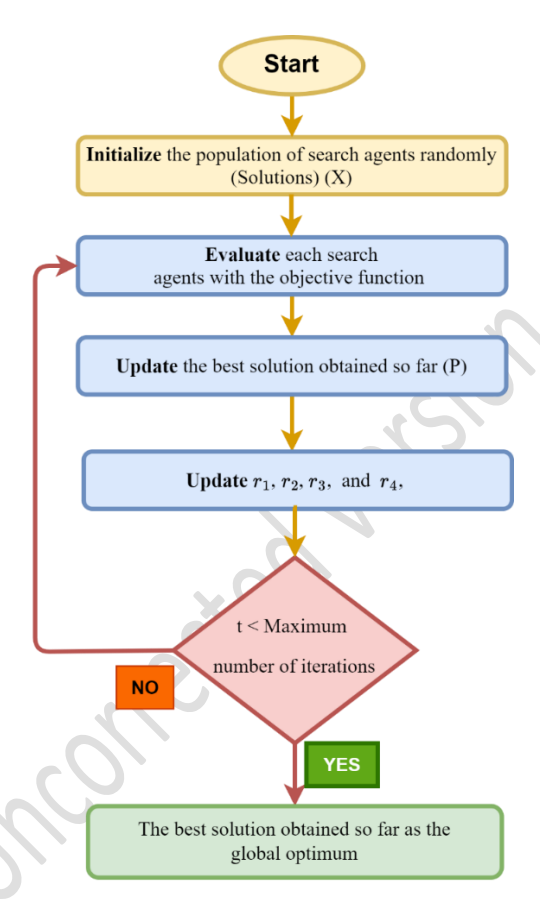


Figure 5. Flowchart of SCA

4 Optimization results and discussion

A step load of 0.1 pu has been applied to the system at t=1, and 10s simulation has been performed.

Repeated debugging can guarantee optimal control performance by determining the search spaces of the controller parameters. The optimum values are obtained using the GWO and SCA due to the specified search spaces provided in Tables 2 and 3

Table 2. Search spaces of the PID+D 2 sliding surface-based controller parameters

Parameter	Search space
k_{sw}	5 - 60
k_1	10 - 100
k_2	0.1 - 70
k_3^2	0.5 - 20
k_{4}^{3}	0.01 - 0.1

Table 3. Search spaces of the Hyperbolic Tangent-based Supertwisting SMC

Parameter	Search space
k_a	0.1 - 5
k_b^{α}	0.1 - 10

4.1 Optimization of PID+D² sliding surface-based controller

In the optimization stage of the controller, the performance of the optimization algorithms is evaluated with varying numbers of iterations. There are five parameters to be optimized in the PID+D 2 sliding surface-based controller. In Tables 4 and 5, the optimization results are obtained with SCA and GWO, respectively. It is clear from the tables that the optimum parameters vary in a large band, while the resultant ISE varies in a narrow band. Bold & italic results indicate the best one in the corresponding table, and system responses are given in Figs. 6 and 7.

When the load is applied at *t*=1s, the PID+D² sliding surface-based controller recovers the frequency deviation immediately.

4.2 Optimization of Hyperbolic Tangent-based Supertwisting SMC

Hyperbolic Tangent-based Super-twisting SMC is tunable with two parameters. The optimal controller parameters are explored with SCA and GWO. The results are given in Tables 6 and 7. Bold & italic results indicate the best one in the corresponding table, and system responses are presented in Figs. 8 and 9.

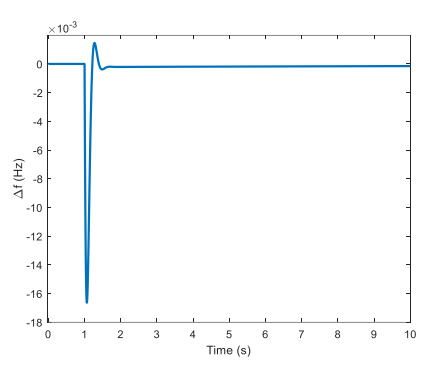


Figure 6. Response of the PID+D² sliding surface-based controller with the SCA-optimized best parameters of Table 4

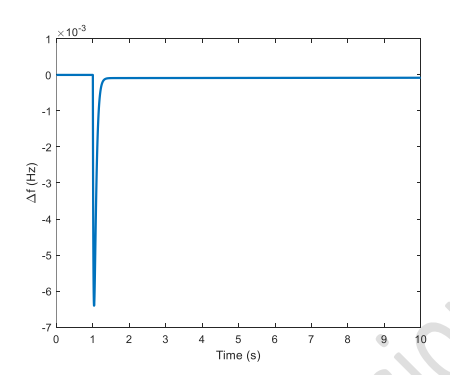


Figure 7. Response of the $PID+D^2$ sliding surface-based controller with the GWO-optimized best parameters of Table 5

Table 4. Optimization results of PID+D2 sliding surface-based controller with SCA

Number of search agents	Iteration number	k_1	k_2	k_3	k_4	k_{sw}	ISE (×10 ⁻³)
20	25	40.0000	51.4346	7.5438	0.0104	22.1013	0.4800
30	25	22.1013	59.3572	4.1994	0.0153	16.7905	0.4113
25	40	38.4343	45,0000	7.7681	0.0318	14.9787	0.4595
30	50	38.6044	49.5735	10.000	0.0414	18.8916	0.5095
20	20	37.1740	37.8087	3.0243	0.0284	16.3577	0.3632
40	30	18.9504	0.45504	2.2082	0.0239	17.5409	0.3602
25	20	18.3862	1.20420	2.2210	0.0100	20.0000	0.3757
30	30	17.7090	1.05010	2.0000	0.0351	19.7646	0.3560
25	40	17.3751	0.70370	1.0823	0.0434	20.0000	0.3322
50	30	16.7119	0.36190	2.2825	0.0103	18.0000	0.3934

Table 5. Optimization results of PID+D² sliding surface-based controller with GWO

	rubic of opumination rotatic of the following current based controller man are						
Number of grey wolfs	Iteration number	k_1	k_2	k_3	k_4	k_{sw}	ISE (×10 ⁻³)
20	25	87.9313	1.0689	6.3081	0.0813	11.9347	0.3274
30	20	76.8929	0.9748	4.9444	0.0680	9.4022	0.3279
50	30	94.5270	0.9502	6.5141	0.0767	10.9089	0.3277
25	25	89.0071	1.2544	6.0810	0.0724	9.9990	0.3276
40	25	49.6900	0.1137	3.5945	0.0509	35.9288	0.3275
30	30	51.7758	0.3512	3.9937	0.0584	43.4482	0.3277
40	50	34.1611	0.5963	2.2332	0.0155	20.0000	0.3277
25	40	54.1647	0.4456	3.8907	0.0534	25.5353	0.3275
25	20	47.3721	0.1752	3.3545	0.0483	30.3545	0.3275
30	20	59.4858	0.3449	4.1234	0.0667	40.0884	0.3279

Table 6. Optimization results of Hyperbolic Tangent-based Super-twisting SMC with SCA

Number of search agents	Iteration number	k_a	k_b	ISE (×10-3)
25	25	0.8000	2.7000	20.48
30	20	0.6420	0.9855	24.27
20	40	0.8000	2.7634	<i>15.63</i>
50	30	0.7455	2.5023	17.98
20	25	0.7000	0.5000	20.48
40	20	0.8000	2.3030	15.64
25	30	0.8000	2.1022	15.65

Table 7. Optimization results of Hyperbolic Tangent-based Super-twisting SMC with GWO

Number of grey wolfs	Iteration number	k_a	k_b	ISE (×10-3)
25	25	0.7000	0.6965	20.47
25	40	0.6912	0.8000	20.99
40	20	0.7710	2.8000	16.81
<i>30</i>	<i>30</i>	0.7869	3.7816	16.12
20	25	0.6000	0.8000	27.75
40	20	0.7000	0.9684	20.46
30	50	0.7000	0.7000	20.47
50	50	0.7000	0.9000	20.46

While the optimum parameters and resultant ISE magnitude vary largely, both optimization algorithms, SCA and GWO, are able to find various combinations of controller parameter magnitudes that give satisfactory output.

The PID+D 2 sliding surface-based controller produced more appropriate control input to reject the applied disturbance than that of Hyperbolic Tangent-based Super-twisting SMC. Because of the oscillatory output, the ISE and ITAE measurements are larger when Hyperbolic Tangent-based Super-twisting SMC used, as seen in Table 8.

As understood from the best ISE magnitudes, the output characteristics of the optimized parameters are nearly the same. On the other hand, the controller parameters are significantly different. All simulation results provide the frequency regulations of Türkiye and the EU.

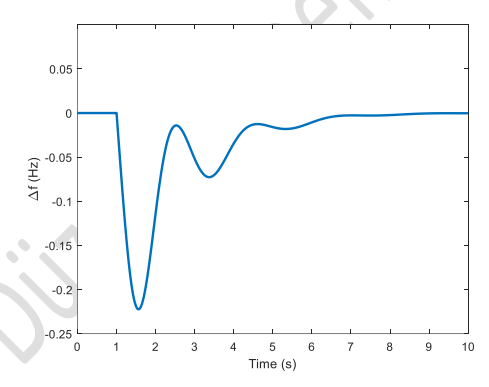


Figure 8. Response of the Hyperbolic Tangent-based Supertwisting SMC with SCA-optimized best parameters of Table $6\,$

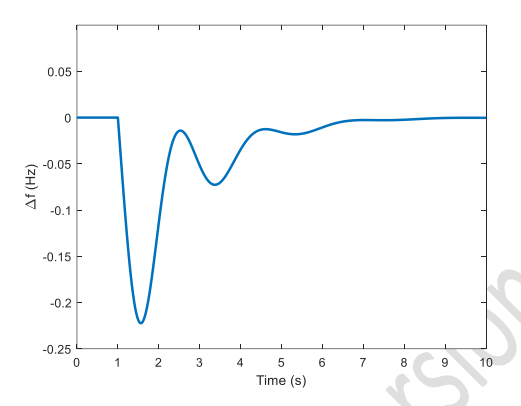


Figure 9. Response of the Hyperbolic Tangent-based Supertwisting SMC with the GWO-optimized best parameters of Table 7

The phase trajectory of the Hyperbolic Tangent-based Supertwisting SMC algorithms is given in Fig. 10. As seen in the figure, the system response oscillates and then stabilizes at the origin.

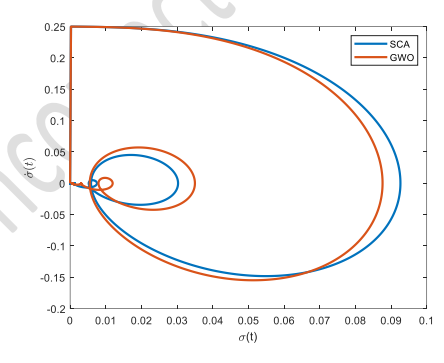


Figure 10. Hyperbolic Tangent-based Super-twisting SMC algorithms' phase trajectories

As expected, the performance of model-based SMC (PID+D 2) is better than the performance of Hyperbolic Tangent-based Super-twisting SMC. Considering the real application of a controller, it is difficult to define an exact model of a system. On the other hand, an approximate model can be used to obtain a control signal. Besides, non-model-based SMC controllers give satisfactory results, as summarized in Table 8.

Table 8. Summary of the controllers' performance

		Under- shoot (Hz)	Over- shoot (Hz)	ISE (×10 ⁻³)	ITAE (×10 ⁻³)
PID+D ² sliding surface-	S C A	-0.0166	0.0014	0.3322	12.5
based control	G W O	-0.0063	0	0.3274	10.4
Hyperbolic Tangent- based	S C A	-0.2223	0	15.63	324.5
Super- twisting SMC	G W O	-0.2096	0	16.12	358.6

In Fig. 11, the responses of the $PID+D^2$ sliding surface-based SCM and the Hyperbolic Tangent-based ST SMC algorithm performance surface are combined to compare clearly. The model-based SMC ($PID+D^2$) rejected the load disturbance better than the Hyperbolic Tangent-based ST SMC. This

advantage depends on the model accuracy of the system used in the controller design. On the other hand, since ST SMC is model-free, an acceptable performance can be obtained by appropriately tuned controller parameters. Both controllers successfully rejected the applied disturbance.

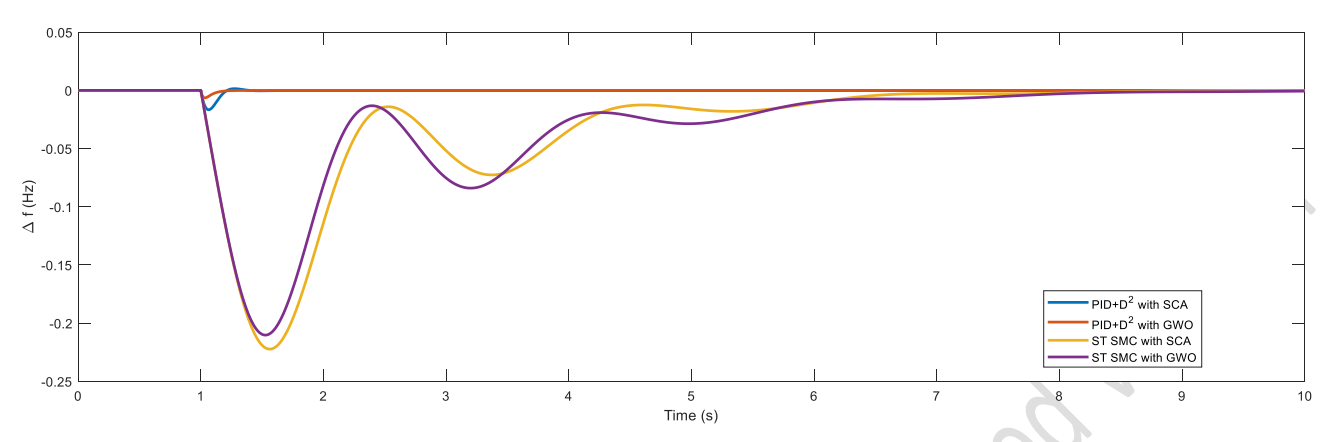


Figure 11. Combined output responses of the controllers optimized with SCA and GWO

5 Conclusions

In this study, a PID+D² sliding surface-based SMC, which incorporates the model of the power system, and a model-free hyperbolic tangent-based ST-SMC algorithm, smoothed with a hyperbolic tangent function, are evaluated for LFC of a SAPS. Both controllers have been paid attention to recently. The optimization of the controllers was performed with SCA and GWO algorithms using ten different numbers of candidate solutions and iterations. All of them gave satisfactory output when a load disturbance was applied.

According to the results, the PID+D²-based SMC generated more desirable output as compared to the ST-SMC. The mathematical model of a real power system and the impacts of disturbances are not straightforward. However, an approximate model can be used in the design of a model-based SMC. Both optimization algorithms gave similar results with different combinations of controller parameters. Therefore, multiple optimal points exist in the search space.

By the nature of super-twisting SMC, damping oscillations were observed when a load disturbance was applied. Acquiring the ST-SMC can be realized more easily, as it does not rely on the mathematical model parameters of the system. This feature of the ST-SMC is the key benefit over model-based SMC algorithms.

Both controllers provided a stable output that satisfied the regulations of Türkiye and the EU.

In the future, a MAPS will be studied for the LFC with new SMCs.

6 Author contribution statement

In this study, both authors conceived the concept of the paper. Author 1 reviewed the literature, performed the simulations, organized and wrote the manuscript, and Author 2 supervised and revised the final version of the manuscript.

7 Ethics committee approval and conflict of interest statement

"There is no ethics committee approval needed for this article".

"In addition, there is no conflict of interest with any person or organization in this article".

8 References

- [1] Abdalla MA, Yang G, Niasse M. "Load frequency regulation of two-area system consisting of PV grid and thermal non-reheated model," in 2021 8th International Forum on Electrical Engineering and Automation, IFEEA 2021, Xi'an, China, 3-5 September 2021.
- [2] European Union, "Commission Regulation (Eu) 2016/631 of 14 April 2016 establishing a network code on requirements for grid connection of generators," 2016.
- [3] T.C. Cumhurbaşkanlığı Mevzuat Bilgi Sistemi. "Elektrik Piyasası Şebeke Yönetmeliği". Available: https://www.mevzuat.gov.tr/mevzuat?MevzuatNo=1972 2&MevzuatTur=7&MevzuatTertip=5 (18.03.2025).
- [4] Khan IA. et al. "Load Frequency Control Using Golden Eagle Optimization for Multi-Area Power System Connected Through AC/HVDC Transmission and Supported With Hybrid Energy Storage Devices," IEEE Access, 11, April, 44672–44695, 2023.
- [5] Hote YV, Jain S. "PID controller design for load frequency control: Past, Present and future challenges," *IFAC-PapersOnLine*, 51, 4, 604–609, 2018.
- [6] Guo J. "Application of a novel adaptive sliding mode control method to the load frequency control," *European Journal of Control*, 57, 172–178, 2021.
- [7] Kumar KV, Kumar TA, Ganesh V. "Chattering free sliding mode controller for load frequency control of multi area power system in deregulated environment," in 2016 IEEE 7th Power India International Conference, PIICON 2016, Bikaner, India, 25-27 November 2016.
- [8] Poulose A, Ramesh Kumar P. "Super-Twisting Algorithm based Load Frequency Control of a Two Area Interconnected Power System," in 2019 20th International Conference on Intelligent System Application to Power Systems, ISAP 2019, New Delhi, India, 10-14 December 2019.
- [9] Guo X, Liu X. "Particle swarm optimization sliding mode control on interconnected power system," in *Proceedings* of the 33rd Chinese Control Conference, CCC 2014, Nanjing, China: TCCT, CAA, 28-30 July 2014.
- [10] Shouran M, Anayi F, Packianather M. "The bees algorithm tuned sliding mode control for load frequency control in two-area power system," *Energies*, 14, 18, 2021.

- [11] Cetinkaya U, Demirbas S, Ayik S, Bayindir R. "Design of Sliding Mode Controller for Load Frequency Control Using Particle Swarm and Grey Wolf Algorithms," in 12th IEEE International Conference on Renewable Energy Research and Applications, ICRERA 2023, Oshawa, Canada, 29 August-1 September 2023.
- [12] Kondo H, Suzuki Y, Iwamoto S. "A load frequency control design using the sliding mode control theory and disturbance observer," in 2010 9th International Power and Energy Conference, IPEC 2010, Suntec, Singapore, 27-29 October 2010.
- [13] Kumar A, Anwar MN, Kumar S. "Sliding mode controller design for frequency regulation in an interconnected power system," *International Journal of Electrical Power and Energy Systems*, 6, 6, 1–12, 2021.
- [14] Sambariya DK, Nagar O. "Application of FOPID Controller for LFC using elephant herding optimization technique," in 2018 3rd IEEE International Conference on Recent Trends in Electronics, Information and Communication Technology, RTEICT 2018 - Proceedings, Bangalore, India, 18-19 May 2018.
- [15] Saka M, Eke I, Gozde H, Taplamacioglu MC. "FO-PID controller design with sca for communication time delayed lfc," *International Journal on Technical and Physical Problems of Engineering*, 12, 4, 63–68, 2020.
- [16] Mohammadikia R, Aliasghary M. "A fractional order fuzzy PID for load frequency control of four-area interconnected power system using biogeography-based optimization," *International Transactions on Electrical Energy Systems*, 29, 2, 1–17, 2019.
- [17] Tan W. "Tuning of PID load frequency controller for power systems," *Energy Conversion and Management*, 50, 6, 1465–1472, 2009.
- [18] Vrdoljak K, Perić N, Petrović I. "Sliding mode based load-frequency control in power systems," *Electric Power Systems Research*, 80(5), 514–27, 2010.
- [19] Deng Z, Chang X. "Frequency Regulation of Power Systems with a Wind Farm by Sliding-Mode-Based Design," IEEE/CAA Journal of Automatica Sinica, PP(99), 1980–89, 2022

- [20] Guo J. "A Novel Proportional-Derivative Sliding Mode for Load Frequency Control," IEEE Access 12(September), 127417–25, 2024.
- [21] Furat M. "Chattering attenuation analysis in variable structure control for automatic voltage regulator with input constraints," *Engineering Science and Technology, an International Journal*, 45, May, 101499, 2023.
- [22] Mohapatra B, Sahu BK, Pati S. "A novel optimally tuned super twisting sliding mode controller for active and reactive power control in grid-interfaced photovoltaic system," *IET Energy Systems Integration*, 5, 4, 491–511, 2023.
- [23] Türksoy Ö, Türksoy A. "A fast and robust sliding mode controller for automatic voltage regulators in electrical power systems," Engineering Science and Technology, an International Journal, 53, March, 2024.
- [24] Li Z, Zhou S, Xiao Y, Wang L. "Sensorless vector control of permanent magnet synchronous linear motor based on self-adaptive super-twisting sliding mode controller," *IEEE Access*, 7, 44998–45011, 2019.
- [25] Huangfu Y, Guo L, Ma R, Gao F. "An Advanced Robust Noise Suppression Control of Bidirectional DC-DC Converter for Fuel Cell Electric Vehicle," *IEEE Transactions on Transportation Electrification*, 5, 4, 1268–1278, 2019.
- [26] Utkin VI. "Variable Structure Systems with Sliding Modes," IEEE Transactions on Automatic Control, AC-22, 2, 212–222, 1977.
- [27] Furat M, Gidemen Cücü G. "Design, Implementation, and Optimization of Sliding Mode Controller for Automatic Voltage Regulator System," *IEEE Access*, 10, 2022.
- [28] Shtessel YB, Shkolnikov IA, Levant A. "Smooth secondorder sliding modes: Missile guidance application," *Automatica*, 43, 1470–1476, 2007.
- [29] Mirjalili S. "SCA: A Sine Cosine Algorithm for solving optimization problems," *Knowledge-Based Systems*, 96, 120–133, 2016.
- [30] Mirjalili S, Mirjalili SM, Lewis A. "Grey Wolf Optimizer," *Advances in Engineering Software Journal*, 69, 46–61, 2014.